

J Therm Anal Calorim (2009) 98:579–589  
DOI 10.1007/s10973-009-0268-0

# Determination of the glass transition temperature

## Methods correlation and structural heterogeneity

John M. Hutchinson

Received: 15 April 2009 / Accepted: 17 June 2009 / Published online: 28 August 2009  
© Akadémiai Kiadó, Budapest, Hungary 2009

**Abstract** The definition of the glass transition temperature,  $T_g$ , is recalled and its experimental determination by various techniques is reviewed. The diversity of values of  $T_g$  obtained by the different methods is discussed, with particular attention being paid to Differential Scanning Calorimetry (DSC) and to dynamic techniques such as Dynamic Mechanical Thermal Analysis (DMTA) and Temperature Modulated DSC (TMDSC). This last technique, TMDSC, in particular, is considered in respect of ways in which the heterogeneity of the glass transformation process can be quantified.

**Keywords** Glass transition · Differential scanning calorimetry · Structural relaxation · Heterogeneity · Vitrification · Glassy state

### Introduction

In any discussion of the glass transition temperature,  $T_g$ , it is important to be clear what is meant by the glass transition itself. The glass transition represents the change that occurs when a system, initially in an equilibrium liquid-like or rubbery state defined by the thermodynamic variables temperature ( $T$ ) and pressure ( $P$ ) (and possibly also by other variables, such as composition in chemically reacting systems), transforms into a non-equilibrium glassy state as a result of a restriction of the molecular mobility

[1], corresponding to an increase in the average relaxation time. The most common circumstance in which this restriction of the molecular mobility leading to a glass transition is observed occurs when the temperature is decreased, hence the use of the term “freezing-in” of the equilibrium structure in the glass. Nevertheless, a glass transition may equally well be observed isothermally, for example by increasing the pressure [1, 2] or during the cross-linking (curing) of a thermosetting system [3], the process in this latter case usually being referred to as vitrification. For the present purposes, however, where we are concerned with the determination of the glass transition temperature, the discussion will be restricted mainly to situations in which the transition occurs on cooling.

It is worth stressing that, in respect of the determination of  $T_g$ , the glass transition region should strictly speaking be traversed on cooling, and not on heating. In simple terms, this is because  $T_g$  defines the temperature at which the liquid-to-glass or rubber-to-glass transition occurs, and not the glass-to-liquid or glass-to-rubber transition. This is not just a question of semantics. Specifically, for any meaningful determination of  $T_g$  it is generally essential that the starting point for the transition be one of equilibrium. This is patently not the case when the starting point is the glassy state which, as will be seen in more detail later, is a function of the whole thermal history since the system was last in equilibrium.

This may seem somewhat paradoxical since a differential scanning calorimeter (DSC), which is routinely used in the determination of  $T_g$ , invariably has the temperature scale calibrated on heating. Indeed, the ASTM Standard Test Method [4] for the determination of  $T_g$  defines this temperature with respect to a DSC heating curve, albeit following a fairly precisely defined previous thermal history involving cooling from an equilibrium state prior to

---

J. M. Hutchinson (✉)  
Departament de Màquines i Motors Tèrmics, ETSEIAT,  
Universitat Politècnica de Catalunya, Carrer Colom 11,  
08222 Terrassa, Spain  
e-mail: hutchinson@mmt.upc.edu

the heating scan in the DSC. The saving grace here is that the heating scan can indeed give a reasonable approximation to  $T_g$  if the cooling and heating rates are not too dissimilar, and that the heating scan begins shortly after the cooling stage finishes.

The transition that takes place on cooling is accompanied by a change from a liquid-like to a glassy structure, and hence can be monitored by any property that is dependent on the structure. Such properties may be thermal (e.g. heat capacity) [5], physical (e.g. specific volume) [6], mechanical (e.g. dynamic modulus) [7], or electrical (e.g. ionic conductivity) [8], amongst others. In respect of thermal properties, the glass transition temperature can then be determined from the mid-point of the sigmoidal change in the heat capacity or from the extrapolated intersection of the asymptotes to the liquid and glassy regions for the enthalpy, as illustrated in Fig. 1. Also shown in this figure is the heating scan immediately

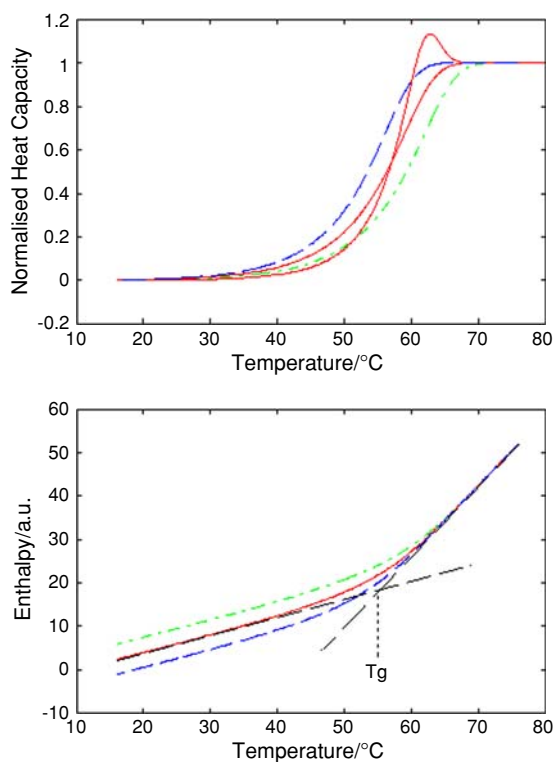


**Fig. 1** Simulated response, as a function of temperature, of a glass-forming material on cooling through the glass transition region at  $-100 \text{ K min}^{-1}$  (green, dash-dotted line),  $-10 \text{ K min}^{-1}$  (red, full line), and  $-1 \text{ K min}^{-1}$  (blue, dashed line). Upper diagram: normalised heat capacity, also showing (red, full line) the response on heating at  $10 \text{ K min}^{-1}$  immediately after cooling at the same rate. Lower diagram: enthalpy in arbitrary units (a.u.), also showing, for  $-10 \text{ K min}^{-1}$ , the construction for the determination of  $T_g$ . TNM model parameters:  $x = 0.4$ ,  $\beta = 0.4$ ,  $\Delta h^*/R = 85 \text{ kK}$

following cooling at the same rate, where it can be seen that, in spite of the hysteresis which is an inherent aspect of the glass transition [9, 10], under these particular circumstances the mid-point temperatures for cooling and heating are essentially the same, as mentioned above in respect of the ASTM Standard Test Method.

Behind this apparently simple procedure for the determination of  $T_g$ , however, lie a number of complications. First, the value of  $T_g$  determined in the manner outlined above is dependent on the cooling rate. Second, different properties, such as those given in the examples above, respond differently to structural changes, and hence the value of  $T_g$  will depend on the choice of property used to detect the transition. This has important implications for the study of physical aging [11–13]. Third, the use of a property such as the dynamic modulus requires a stimulus in order to provide the response from which  $T_g$  is determined. This introduces another variable (in this case, frequency) upon which the value of  $T_g$  depends, and introduces the interesting relationship between cooling rate and frequency [14–19]. These aspects, as well as additional information about the glass transformation process that can be obtained from the determination of  $T_g$ , are discussed in this paper.

## Determination of $T_g$

### Fictive temperature

If we consider isobaric conditions and stable systems in which no chemical reactions are occurring, then the glass transition occurs on cooling, and the glass transition temperature depends on the cooling rate, as shown in Fig. 1 for the case of enthalpy measurements. In fact, the mid-point temperature on cooling, for any given cooling rate, is slightly higher than  $T_g$  determined from the enthalpy plot. The reason for this is that the cooling curve for the heat capacity is not symmetric about the mid-point: the more non-linear is the response (lower values of non-linearity parameter,  $x$ , to be defined shortly), the more asymmetric is the cooling curve and the greater is the difference between the mid-point temperature and  $T_g$ . This can be rationalised through the use of the fictive temperature,  $T_f$ .

The fictive temperature is a concept first introduced by Tool [20] for the purposes of describing structural relaxation in glass, and is defined as the temperature at which a glass would appear to be in equilibrium if it were instantaneously removed to that temperature. The usual procedure for determining the fictive temperature is by the “equal areas” method [21, 22], illustrated in

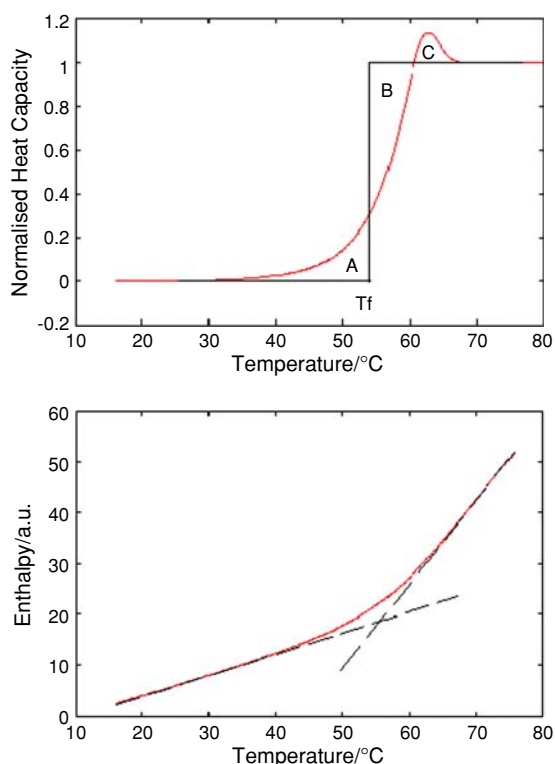


**Fig. 2** Schematic illustration of procedure for determination of fictive temperature,  $T_f$ . The fictive temperature is defined as that temperature for which the sum of the areas A + C is equal to the area B. Upper diagram: normalised heat capacity, showing the response on heating at  $10 \text{ K min}^{-1}$  immediately after cooling at the same rate. Lower diagram: enthalpy in arbitrary units (a.u.) showing, for  $-10 \text{ K min}^{-1}$ , the determination of  $T_g$ . TNM model parameters:  $x = 0.4$ ,  $\beta = 0.4$ ,  $\Delta h^*/R = 85 \text{ kK}$

Fig. 2 for the case of a heating curve which has been made immediately after cooling. Under these particular circumstances, in which heating immediately follows cooling, the fictive temperature is identical to the glass transition temperature. There are two principal advantages of the concept of fictive temperature. First, it can define the state of the glass, not only immediately after cooling, which is what the glass transition temperature defines, but also after whatsoever thermal history. Very often this thermal history involves cooling to a temperature within the glassy state and then annealing at constant temperature, which gives rise to the widely studied phenomenon of structural relaxation [23] or physical aging [11–13], the analysis of which makes use of the fictive temperature of the glass as a function of the aging time. The second advantage is that  $T_f$ , and hence  $T_g$  if the heating scan takes place immediately after cooling, can be determined from a heating scan in the DSC, which is the usual mode of operation.

## Relaxation time

The average relaxation time determines the occurrence of the glass transition. It is commonly assumed that the average relaxation time,  $\tau$ , depends on both temperature,  $T$ , and fictive temperature,  $T_f$ , one of the most widely used expressions to describe this dependence being attributed to Tool [20], Narayanaswamy [24] and Moynihan [22] (TNM):

$$\begin{aligned} \tau(T, T_f) &= \tau_0 \exp \left[ \frac{x\Delta h^*}{RT} + \frac{(1-x)\Delta h^*}{RT_f} \right] \\ &= \tau_g \exp \left[ \frac{x\Delta h^*}{RT} + \frac{(1-x)\Delta h^*}{RT_f} - \frac{\Delta h^*}{RT_g} \right] \end{aligned} \quad (1)$$

In this equation,  $\tau_0$  is a pre-exponential factor,  $\tau_g$  is the average relaxation time in equilibrium at  $T_g$ ,  $x$  is the non-linearity parameter and  $\Delta h^*$  is the apparent activation energy at  $T_g$ . Although this equation gives an Arrhenius temperature dependence for the equilibrium relaxation time whereas it is usually considered to be non-Arrhenius, such as Vogel–Fulcher–Tammann [25–27], this is an acceptable approximation within the narrow temperature interval around the glass transition, hence the use of the term “apparent” for the activation energy. The very large values of  $\Delta h^*/R$  often found, particularly for polymer glasses, can be attributed to the co-operativity of molecular motion in these systems, while the very small values for  $\tau_0$ , often considered unphysical, arise simply from applying an Arrhenius equation to fragile glass-forming systems [28–30], as has been explained elsewhere [31].

Other expressions than Eq. 1 may also be used to describe the dependence of  $\tau$  on temperature and structure (fictive temperature), for example the Adam-Gibbs equation [32] or its more recent modification [33], based upon the concept of configurational entropy [34], or equations based upon free volume [35]. The approximate equivalence of these approaches has been reviewed [36], and relationships between the various parameters have been established [23].

## Effect of cooling rate

The dependence of  $T_g$  on cooling rate,  $q$ , can be derived from the equation describing the temperature and structure dependence of the average relaxation time. For example, from Eq. 1 one obtains:

$$\frac{d \ln |q|}{d(1/T_g)} = -\frac{\Delta h^*}{R} \quad (2)$$

For typical values of apparent activation energy and  $T_g$  for polymers, this equation implies a change of about 3 to 4 K per decade of cooling rate, as can be seen in Fig. 1. By

DSC it is possible to control the cooling rate over about three decades without involving excessive experimental time, and is a preferred method for the determination of the apparent activation energy [37, 38]. The experimental procedure is to cool the sample, initially in an equilibrium liquid state above  $T_g$ , at a controlled rate down to a lower temperature within the asymptotic glassy region, and then immediately to heat at a controlled rate through the transition region. From the heating scan one can determine the fictive temperature, which is the same as the  $T_g$  corresponding to the previous cooling rate, since no annealing took place at the lower temperature. Although in principle the same value of  $T_f$  should be obtained whatever the heating rate, it is best in practice always to use the same rate, typically  $10 \text{ K min}^{-1}$ , for reasons of calibration and thermal lag in the sample [39].

### Methods correlation

#### Volume relaxation and dilatometric $T_g$

The above considerations indicate that, strictly speaking, any value of  $T_g$  that is determined experimentally should specify the appropriate cooling rate. In addition, though, this situation is further complicated by the possibility of using techniques other than DSC, the technique to which most of the foregoing discussion has referred, for the determination of  $T_g$ . Apart from dynamic techniques, to be discussed later, the other classical way of determining  $T_g$  is by dilatometry. Mainly for experimental reasons, though, since the pioneering work of Kovacs on volume relaxation half a century ago [6, 40], dilatometry has largely been superseded by DSC. Nevertheless, there are some notable exceptions, most recently from the groups of Rychwalski [41, 42] and Malek [43–46], in which dilatometry has been used to study volume relaxation. The comparison of volume and enthalpy relaxation rates is interesting in respect of observing how the different properties respond to the structural changes occurring at the glass transition, but it remains controversial. Many authors report that equilibrium relaxation times are longer for enthalpy than for volume relaxation [47–49], while others suggest that, at least within the limited temperature interval in which equilibrium can be achieved on an experimental time scale, there is no significant difference between the equilibrium relaxation times for volume and enthalpy [42, 46, 50–52].

This controversy well illustrates all the important features related to the determination of the glass transition temperature. First, calorimetric and dilatometric experiments typically involve different cooling rates (e.g.  $\sim 10\text{--}20 \text{ K min}^{-1}$  for calorimetry and  $\sim 1 \text{ K min}^{-1}$  and less for dilatometry) for glass formation, and hence

different  $T_g$  values unless proper attention is paid to the rate dependence of  $T_g$ . This is important if inferences about relaxation rates are drawn from isothermal relaxation either at a given temperature or at a given temperature difference below  $T_g$ . Second, there is no a priori reason why enthalpy and volume should respond in the same way to structural changes in the glass-forming system, and hence may not have the same  $T_g$  even for a given cooling rate. And third, the apparent activation energy, which defines the cooling rate dependence of  $T_g$  through Eq. 2, is generally found to be different for enthalpy and volume relaxation, so that even if they have the same  $T_g$  for a given cooling rate, then at temperatures below  $T_g$  their equilibrium relaxation times will diverge. Thus, for example, using the TNM equation to model relaxation data for polystyrene, one can find reports of both a higher apparent activation energy for volume than for enthalpy [52] as well as the opposite result [42]. This particular discrepancy is probably due to the inability of the TNM model to adequately describe the relaxation behaviour. Interestingly, on the other hand, a recent study of polyvinyl acetate [46] finds a single set of TNM parameter values for both enthalpy and volume relaxation, implying the same kinetics for both measurement methods.

#### Dynamic methods of determining $T_g$

Dynamic methods, such as Dynamic Mechanical Thermal Analysis (DMTA) and Dielectric Analysis (DEA), are commonly used in the study of relaxations in polymers [7]. Over a wide temperature range, a number of different transitions are often observed, and conventionally they are denoted as the  $\alpha$ -,  $\beta$ -,  $\gamma$ -, etc. relaxations in order of decreasing temperature. For glassy polymers, the  $\alpha$ -relaxation determined by DMTA is associated with the glass transition e.g. [53], and involves a relatively sharp change in dynamic modulus of about three decades and a pronounced peak in the loss tangent,  $\tan \delta$ . The detection of a glass transition is much more sensitive by DMTA than by DSC, and hence for some systems in which the glass transition is weak DMTA is the preferred method for analysis. However, one should be clear about what is being determined by DMTA.

As pointed out earlier, there are two time scales involved in any dynamic method: one is associated with the applied cooling rate used to traverse the transition region, and the other is associated with the frequency of the applied stimulus. This observation is appropriate even under isothermal conditions, for which one can determine, by DMTA for example, the frequency dependence of the peak in  $\tan \delta$ , which may be interpreted as the frequency dependence of  $T_g$  [54–56]. The reason for this is that the isothermal temperature must be approached following some previous thermal history, which for studies of the

glass transition usually involves cooling from an equilibrium state above  $T_g$ . Hence the glassy state for the isothermal DMTA measurements is determined by this cooling rate and the subsequent aging time at the isothermal temperature. Thus the value of  $T_g$  obtained by DMTA and associated with the peak in  $\tan \delta$ , for which  $\omega\tau = 1$ , where  $\omega$  is the angular frequency and  $\tau$  is the average molecular relaxation time, depends not only on the frequency  $\omega$  but also on the average relaxation time  $\tau$ , which is a function of the cooling rate and aging time. Furthermore, it has been suggested [57] that in regions of high damping, in other words at the peak in  $\tan \delta$ , the energy required to be dissipated as a result of the forced vibrations of DMTA actually modifies (rejuvenates [11]) the glassy state, and hence has an influence on the evolution of the dynamic mechanical properties, and that a better approach would be to determine the logarithmic decrement [7] by means of a torsional pendulum or equivalent.

The situation is more complex than might at first appear, therefore. Strictly speaking, the peak in  $\tan \delta$  measured by DMTA represents the  $\alpha$ -relaxation. For amorphous polymers, this can be associated with the glass transition, but in view of the frequency dependence of the temperature at which the peak occurs, it would be better to refer to this as a dynamic glass transition. Nevertheless, for the frequency range usually used in DMTA ( $\sim 0.1$ – $100$  Hz), the dynamic  $T_g$  values thus found are reasonable close to the calorimetric  $T_g$  values obtained by DSC using typical cooling rates. This is not the case for DEA, for which the frequency range is much higher, typically from about  $10^2$  to  $10^5$  Hz, and hence which gives rise to peaks in the dielectric loss factor,  $\epsilon''$ , at temperatures significantly higher than the calorimetric  $T_g$ . For this reason, for DEA in particular, it would be preferable to refer to such peaks arising from the  $\alpha$ -relaxation rather than the glass transition, though this distinction is not always appreciated [58].

An excellent illustration of the distinction between the glass transition and the  $\alpha$ -relaxation is afforded by studies of the vitrification process that occurs during the isothermal curing of thermosets at a cure temperature  $T_c$  below the  $T_g$  of the fully cured system,  $T_{g\infty}$ . Under such circumstances, the glass transition temperature of the curing system increases as the degree of cross-linking increases, at a rate controlled by the chemical reaction, until it approaches  $T_c$ . The rate of reaction then slows down dramatically, since it is now controlled not by the chemical reaction but by the diffusion of the reacting species, which is very slow as the system is vitrifying. The vitrification time  $t_v$  at a given  $T_c$  is usually taken to be the time when the  $T_g$  of the curing system is equal to  $T_c$ . By conventional DSC it is not possible to follow in real time the development of  $T_g$  during isothermal cure, and hence the study of the isothermal vitrification process by conventional DSC involves a time-

consuming series of determinations of  $T_g$  as a function of cure time [3, 59].

On the other hand, Temperature Modulated DSC (TMDSC) does provide an indication in real time of the vitrification process, through the complex heat capacity,  $C_p^*$ , discussed in more detail below. When vitrification occurs, there is a sigmoidal change in  $C_p^*$  from a value characteristic of a liquid to one characteristic of a glass, the mid-point usually being used to identify the vitrification time,  $t_v$  [60–64], analogous to the determination of the dynamic glass transition temperature by TMDSC on cooling [65, 66]. It is clear, though, that the vitrification time determined by TMDSC is frequency-dependent, similar to the peak in  $\tan \delta$  determined by DMTA and discussed above, and that this arises from the distinction between the glass transition and the  $\alpha$ -relaxation [67, 68]. As for DMTA, though, the typical frequency range used in TMDSC (modulations periods from about 30 to 300 s) results in this distinction not being excessive. In contrast, when the vitrification time is determined by DEA, this distinction is much more important in view of the higher frequencies involved, and should be taken into consideration.

#### Determination of $T_g$ by temperature modulated DSC

Unlike the dynamic techniques of DMTA and DEA considered above, TMDSC permits the comparison of the determination of  $T_g$  by DSC with a dynamic technique for which the stimulus is also a change in temperature. This provides further insight into the distinction between the dynamic and conventional glass transition temperatures. Although, as for DSC, the most common way of using TMDSC to study the glass transition is on heating, for simplicity we will discuss here the situation on cooling through the transition region. This avoids the complexity associated with aging effects.

A schematic illustration of the determination of  $T_g$  by TMDSC is shown in Fig. 3, for simulations made using the TNM parameter values  $x = 0.4$ ,  $\beta = 0.4$  and  $\Delta h^*/R = 80$  kK, and for experiments with an underlying cooling rate of  $-0.25$  K  $\text{min}^{-1}$  from 393 to 353 K, an amplitude of temperature modulation of 0.5 K, and modulations periods of 12, 30, 60, 120 and 300 s. A relaxation time of 100 s in equilibrium at 373 K is assumed in order to define the glass transition region, and liquid and glassy specific heat capacities of 1.6 and 1.3 J  $\text{g}^{-1}$   $\text{K}^{-1}$  are assumed, respectively. The upper diagram presents the in-phase specific heat capacity,  $C_p'$ , almost identical to the complex specific heat capacity,  $C_p^*$ , while the lower diagram presents the average specific heat capacity,  $C_{p,\text{ave}}$ , equivalent to a DSC curve at the same cooling rate,  $-0.25$  K  $\text{min}^{-1}$  in the present case. The thickening of the  $C_{p,\text{ave}}$  trace, most noticeably at the

onset of the transition, is caused by ripples arising from the Fourier Transform procedure, which is also responsible for the unevenness of the  $C_p'$  traces, particularly for the longer modulation periods [17, 69–71].

The glass transition is manifest in TMDSC as a sigmoidal change in the  $C_p'$  (and  $C_p^*$ ) trace (and by a negative peak in the out-of-phase specific heat capacity,  $C_p''$ , and in the phase angle,  $\phi$ ), as seen in the upper diagram of Fig. 3, from which a dynamic  $T_g$  can be determined, for example as the mid-point temperature. This is clearly dependent on the period, or frequency, of the modulations, increasing with increasing frequency, and for the conditions selected here is always greater than the mid-point  $T_g$  determined from the  $C_{p,ave}$  trace in the lower diagram of Fig. 3, sometimes referred to as the thermal transition. Two other important aspects should be noted, however.

First, the dynamic transition is much sharper than the thermal transition. This is clearly seen by the complete change from a liquid-like value to a glassy value for  $C_p'$ , whereas  $C_{p,ave}$  never reaches the asymptotic glassy state within the temperature range used. The reason for this is that  $C_p'$  represents essentially a quasi-equilibrium relaxation, and hence the transition width depends (ideally)

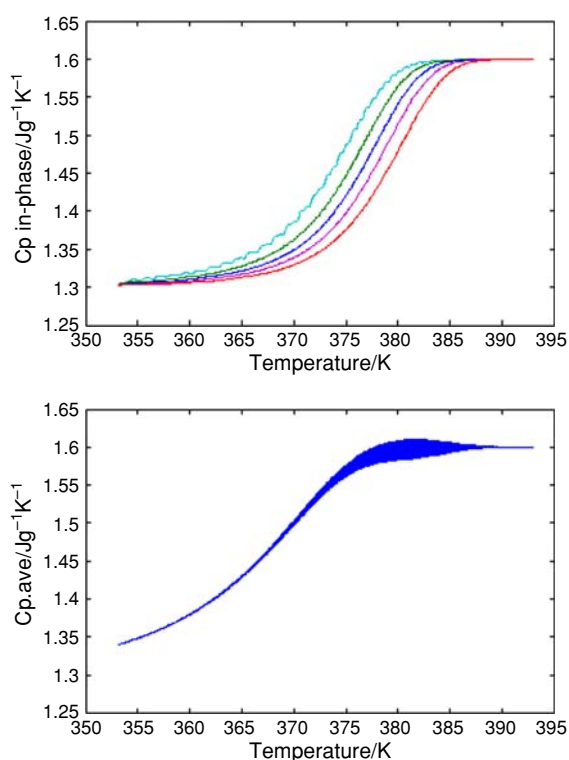


**Fig. 3** Simulated response of TMDSC to cooling through the glass transition region. Upper diagram: in-phase specific heat capacity, with modulation periods of 300, 120, 60, 30 and 12 s, decreasing from left to right. Lower diagram: average specific heat capacity, for modulation period of 12 s

only on the distribution of relaxation times, defined by the KWW exponent  $\beta$ , and not on the non-linearity parameter,  $x$  [17, 72]. On the other hand, the thermal transition evidenced by  $C_{p,ave}$  certainly does involve a departure from equilibrium, and is therefore dependent on both  $\beta$  and  $x$ , becoming increasingly broad as  $x$  decreases. This is a very clear indication of the different natures of the dynamic and thermal transitions.

The strict condition for the dynamic transition to be quasi-equilibrium is that it be wholly separated on the temperature scale from the thermal transition. In practice this is a difficult condition to fulfil by TMDSC, and this is the second important aspect to be noted from Fig. 3. Here it can be seen that, even for the most extreme case, namely the period of 12 s, the thermal transition begins to intervene before the dynamic transition is complete. For longer modulation periods, this overlap becomes more pronounced. One consequence of this is to introduce a certain error into the determination of  $\Delta h^*$  from the dependence of the dynamic  $T_g$  on the frequency [73]. For example, from the results presented in Fig. 3 it is possible to estimate  $\Delta h^*/R$  as approximately 88 kK, whereas the model input value used was 80 kK. There are two approaches for trying to overcome this problem: reducing the modulation period and reducing the underlying cooling rate. For the former there is an experimental limit, about 30 s, below which the sample cannot follow the temperature modulations accurately. Even though a recently introduced novel multi-frequency technique, TOPEM [74], reduces this limit considerably, there is still only a limited frequency interval in which the separation of dynamic and thermal transitions can be considered sufficient. The latter approach, reducing the underlying cooling rate, leads to unacceptably long experimental times. The conditions applying to Fig. 3, for example, imply nearly 3 h for a single cooling scan.

One conclusion to be drawn from these observations is that considerable care should be exercised in the choice of experimental conditions for the determination of the dynamic  $T_g$  by TMDSC. Another is that there must be a relationship between the cooling rate ( $q$ ) and frequency ( $f$ ) required in order to obtain the same  $T_g$  value by DSC and TMDSC, respectively. Such a relationship was proposed originally by Donth and co-workers [18, 75], based upon the fluctuation dissipation theorem of the glass transition:

$$\omega = 2\pi f = \frac{|q|}{a\delta T} \quad (3)$$

where  $\omega$  is the angular frequency,  $a$  is a constant, and  $\delta T$  is the mean temperature fluctuation of the co-operatively rearranging regions, which can be obtained from the dispersion of the relaxation as the width at half-height of the peak in  $C_p''$ . This approach has been applied, principally by Schick and co-workers [14, 16, 76] but also by others

[15, 17, 19, 71, 75], to a wide variety of glass-forming systems. Although there are some discrepancies between the results presented and the theoretical predictions, which may be a consequence of inadequacies in the TNM formulation [77, 78], this avenue appears promising. One particular aspect is that it is possible to estimate [79], from  $\delta T$ , a mean correlation length for co-operatively rearranging regions at the glass transition, which is of considerable current interest in respect of the effects of confinement on relaxation kinetics.

### Structural heterogeneity

It has been appreciated for many years that two fundamental aspects can be attributed to the glass transformation process. The first is that the relaxation kinetics are non-linear, which can be expressed formally, for example, by the inclusion of both temperature  $T$  and fictive temperature  $T_f$  in the equation for the relaxation time (Eq. 1). The second is that a distribution of relaxation times must be included in any analysis, which may be done in a number of ways.

One approach is to consider that all states of the system are determined by the intensive thermodynamic parameters ( $T$  and  $P$ ) and by a set of ordering parameters  $\xi_i$  ( $i = 1:N$ ), as in the KAHR model [80]. The volumetric or enthalpic state of the system at any time may then be described in terms of the discrete distribution of excess volume or enthalpy, each element in this distribution relaxing according to its own current relaxation time,  $\tau_i$ , but for which this relaxation time depends on the global or overall state of the system. This last requirement implies a coupling of each element in the system to the global state, and hence ensures thermorheological simplicity. The advantage of this approach is that it is highly transparent, in that the heterogeneity of the system can be identified at any time simply by viewing the current distribution of excess volume or enthalpy. Although it has recently become fashionable to make reference to *dynamic heterogeneity* in glass-forming systems, this is really no different from the heterogeneity that can be clearly seen in the KAHR model, the development of which can easily be followed throughout any relaxation process. The disadvantage of this approach lies in the mathematical complexity, and in the intractability of a distribution of relaxation times in the comparison with experimental results.

An alternative, and very popular, approach is to make use of the KWW stretched exponential function:

$$\phi(t) = \exp\left[-\left(\frac{t}{\tau}\right)^\beta\right] \quad (4)$$

This expression, in which the exponent  $\beta$  ( $0 \leq \beta \leq 1$ ) is inversely related to the width of the distribution of

relaxation times, provides a mathematically convenient way of introducing a distribution into the relaxation kinetics. The disadvantage is the lack of transparency, inasmuch as this approach gives only an overall view of the relaxation process, and one loses sight of the detailed changes in the heterogeneity of the system as a function of time during any relaxation. Nevertheless, it is generally adopted as the preferred method of introducing a distribution of relaxation times into the analysis, and as a consequence this aspect of the glass transformation behaviour is commonly known as non-exponentiality.

Further support for this non-exponential approach comes from the coupling model, first suggested by Ngai [81, 82]. The argument is that the relaxation of a *primitive species* is coupled to its surroundings, the strength of the coupling being determined by a coupling parameter,  $n$  ( $0 \leq n \leq 1$ ), which increases with increasing strength of the coupling [83]. It can be shown that this model leads to a stretched exponential decay function, such as that in Eq. 4, in which the exponent  $\beta$  is identified as  $(1 - n)$ , and thus gives a physical basis for the phenomenological KWW expression.

The question of whether the relaxation process at the glass transition is distributed as a result of multiple exponential processes or whether it is inherently non-exponential is one which has been asked frequently over many years, and still remains controversial [84]. Nevertheless, the heterogeneous character of molecular dynamics in the glass transition region has been demonstrated experimentally [85, 86], while broadband dielectric spectroscopy has even indicated the existence of heterogeneities far above  $T_g$  [87]. The heterogeneity may be understood in terms of a time scale, involving a distribution of relaxation times, or of a length scale, where the heterogeneities are related to the cooperatively rearranging regions proposed in the theory of Adam and Gibbs [32].

For a distribution of relaxation times, a convenient way of characterising the structural heterogeneity of a glass-forming system in the glass transition region is therefore through the evaluation of the non-exponentiality parameter  $\beta$ . This can be seen qualitatively from a consideration of the width of the glass transition region, a wider transition implying a lower value of  $\beta$  and a broader distribution of relaxation times. This is illustrated in Fig. 4, where the effect of decreasing  $\beta$ , whilst maintaining all the other parameters constant, is clearly seen as a broadening of the transition region. The inflectional tangent drawn for the case of  $\beta = 0.2$  indicates a transition breadth of about 30 K, for example.

However, the measurement of the transition breadth determined by conventional DSC does not give a reliable measure of the heterogeneity of the transformation process, because the kinetics of the transition are affected also by

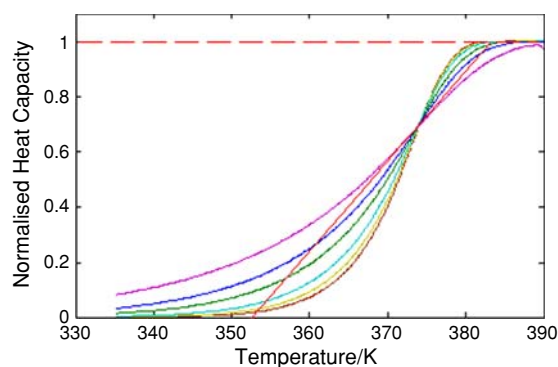


**Fig. 4** Simulated DSC curves on cooling through the glass transition region at  $-10 \text{ K min}^{-1}$ , showing the effect of the non-exponentiality parameter:  $\beta = 0.2, 0.3, 0.4, 0.6, 0.8$  and  $1.0$  as transition width decreases. Other TNM parameters:  $\Delta h^*/R = 80 \text{ kK}$  and  $x = 0.4$ . Inflectional tangent is shown for  $\beta = 0.2$

the non-linearity parameter  $x$ . This is well illustrated in Fig. 5, where simulations of the glass transition on cooling have been made, similar to those in Fig. 4, but in this case showing the effect of decreasing the value of  $x$  whilst maintaining all the other parameters, in particular  $\beta$ , constant. Here it can be seen that decreasing  $x$  increases the breadth of the transition, similar to the effect of  $\beta$ , though to a slightly lesser extent. The inflectional tangent drawn for the case of  $x = 1.0$  indicates a transition breadth of about 15 K, while the breadth for  $x = 0.2$  is about 20 K, for example.

Thus in conventional DSC the effects of non-exponentiality and non-linearity combine in their influence on the breadth of the transition, and hence this breadth cannot be used as a direct measure of the heterogeneity of the system. Temperature Modulated DSC, on the other hand, can

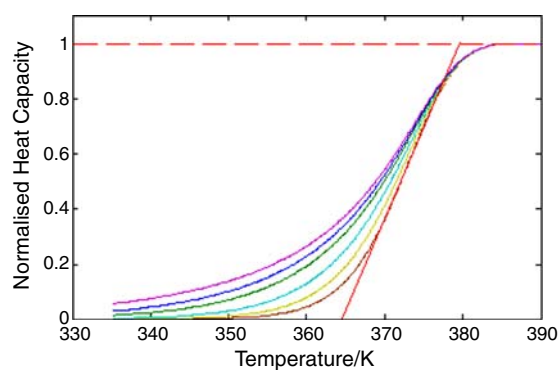


**Fig. 5** Simulated DSC curves on cooling through the glass transition region at  $-10 \text{ K min}^{-1}$ , showing the effect of the non-linearity parameter:  $x = 0.2, 0.3, 0.4, 0.6, 0.8$  and  $1.0$  from left to right as transition width decreases. Other TNM parameters:  $\Delta h^*/R = 80 \text{ kK}$  and  $\beta = 0.4$ . Inflectional tangent is shown for  $x = 1.0$

provide this information. This is because the complex or in-phase specific heat capacity, on cooling through the transition region and under ideal experimental circumstances in which the dynamic glass transition is separated from the thermal transition, is essentially independent of the non-linearity parameter  $x$  but strongly dependent on the non-exponentiality parameter  $\beta$  [17]. Based upon this observation, a new method has been proposed for the experimental determination of  $\beta$  by TMDSC [72].

The length scale attribution of heterogeneity may be understood in terms of the fluctuation dissipation theory of Donth et al. [18, 75], discussed above in respect of the relationship between cooling rate and frequency. According to this theory, the width of the peak in the out-of-phase specific heat capacity,  $C_p''$ , determined by TMDSC is a measure of the temperature fluctuations,  $\delta T$ , in local subsystems. In particular, the peak width at half height is equal to  $2\delta T$  [88]. From the measurement of  $\delta T$ , the volume  $V$  of the subsystem is then found as [79, 89]:

$$V = \frac{kT^2\Delta(1/c_v)}{(\rho\delta T^2)} \quad (5)$$

where  $k$  is Boltzmann's constant,  $\Delta(1/c_v)$  is the change, through the transition, in the reciprocal of the specific heat capacity at constant volume, and  $\rho$  is the density. Finally, the characteristic length,  $\xi$ , is then calculated from  $\xi^3 = V$ .

What measurement best determines the heterogeneity of the glass-forming system is open to debate. It has been suggested that the dispersion of the relaxation time spectrum is a better measure of the temperature fluctuations in local subsystems than is the width of the peak in  $C_p''$  [90]. However, simulations using the TNM equation and the KWW stretched exponential function suggest that, in fact, these two measurements provide the same information. To

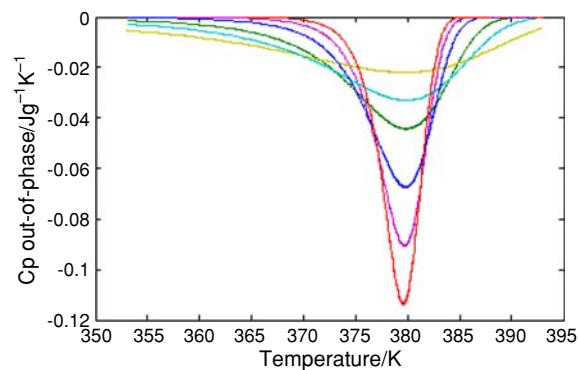


**Fig. 6** Out-of-phase specific heat capacity obtained by simulation of TMDSC cooling experiments at  $-0.25 \text{ K min}^{-1}$  with period = 12 s and  $A_T = 0.5 \text{ K}$ . TNM parameter values:  $x = 0.4$ ,  $\Delta h^*/R = 80 \text{ kK}$ . Non-exponentiality parameter  $\beta = 0.2, 0.3, 0.4, 0.6, 0.8$  and  $1.0$ , in order of increasing peak height

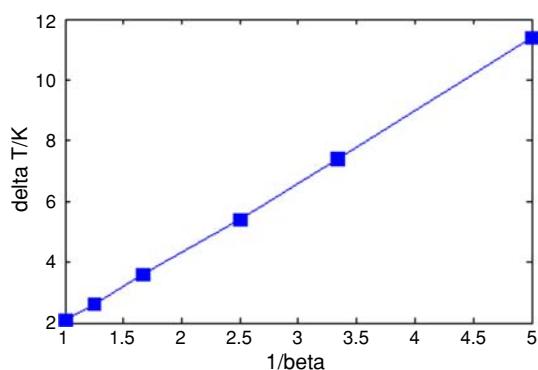


**Fig. 7** Plot of  $\delta T$  versus  $1/\beta$ , using results from Fig. 6

illustrate this, Fig. 6 shows the variation of  $C_p''$  obtained by simulation of a TMDSC cooling experiment at  $-0.25 \text{ K min}^{-1}$  with a period of 12 s and an amplitude of temperature modulations of 0.5 K, and for various values of  $\beta$ . It can clearly be seen that the peak width increases as  $\beta$  decreases. Taking  $\delta T$  as half of the peak width at half height, it is possible to examine the relationship between  $\delta T$  and  $\beta$  predicted by these simulations. In particular, if we assume that the inverse of  $\beta$  is proportional to the width of the distribution of relaxation times, then a plot of  $\delta T$  as a function of  $1/\beta$  will indicate the correspondence between the mean temperature fluctuations and the width of the distribution of relaxation times. This is shown in Fig. 7, where a perfect linear correlation is observed.

### Concluding remarks

The well known dependence of the glass transition temperature on the cooling rate should not detract from the ability to determine  $T_g$  in a precise and well defined way. This can be done calorimetrically by DSC, for example, in which case  $T_g$  should strictly be determined as the fictive temperature,  $T_f$ , from a heating scan performed immediately after cooling through the transition region at a controlled rate, the value determined in this way being referred to the controlled cooling rate used. Nevertheless, for many practical purposes it is sufficient to make use of the ASTM standard method.

On the other hand, it should be borne in mind that techniques other than calorimetric, such as dilatometric, will not necessarily give the same value of  $T_g$ , even for identical cooling rates. Likewise, dynamic techniques such as DMTA or TMDSC will also give different values for the transition temperature, which should preferably be referred to as a dynamic  $T_g$  and which depends on the frequency of the measurement as well as the thermal history.

Finally, the heterogeneity of the glass transformation process gives rise to a broadening of the transition, which can be observed, though only qualitatively, in a conventional DSC scan. The heterogeneity is best quantified through the dynamic response, in particular by TMDSC, from which an estimate of the characteristic length scale associated with the glass transition may be obtained.

### References

1. Rehage G, Borchard W. The thermodynamics of the glassy state. In: Haward RN, editor. The physics of glassy polymers. Barking: Applied Science Publishers; 1973. p. 54–107.
2. McKinney JE, Simha R. Thermodynamics of the densification process for polymer glasses. *J Res Nat Bur Std.* 1977;81A:283–97.
3. Montserrat S. Vitrification and further structural relaxation in the isothermal curing of an epoxy resin. *J Appl Polym Sci.* 1992; 44:545–54.
4. ASTM D3418-08. Standard Test Method for Transition Temperatures and Enthalpies of Fusion and Crystallization of Polymers by Differential Scanning Calorimetry; 2008.
5. Wunderlich B. The basis of thermal analysis. In: Turi EA, editor. Thermal characterization of polymeric materials. Orlando: Academic Press Inc; 1981. p. 91–234.
6. Kovacs AJ. Transition vitreuse dans les polymers amorphes. *Etude phénoménologique.* *Fortschr Hochpolym Forsch.* 1963;3: 394–507.
7. McCrum NG, Read BE, Williams G. Anelastic and dielectric effects in polymeric solids. New York: Wiley; 1963.
8. Hutchinson JM, Ingram MD, Robertson AHJ. The effects of pressure and densification on ionic conductivities in silver iodomolybdate glasses. *Phil Mag B.* 1992;66:449–61.
9. Hutchinson JM, Kovacs AJ. Effects of thermal history on structural recovery of glasses during isobaric heating. *Polym Eng Sci.* 1984;24:1087–103.
10. Hutchinson JM, Ruddy M. Thermal cycling of glasses. 2. Experimental evaluation of the structure (or non-linearity) parameter  $x$ . *J Polym Sci Polym Phys.* 1988;26:2341–66.
11. Struik LCE. Physical aging in amorphous polymers and other materials. Amsterdam: Elsevier; 1978.
12. Hutchinson JM, Bucknall CB. Effects of thermal history on the density and mechanical properties of poly(methyl methacrylate). *Polym Eng Sci.* 1980;20:173–81.
13. Hutchinson JM. Physical aging of polymers. *Prog Polym Sci.* 1995;20:703–60.
14. Hensel A, Dobbertin J, Schawe JEK, Boller A, Schick C. Temperature modulated calorimetry and dielectric spectroscopy in the glass transition region of polymers. *J Therm Anal.* 1996;46:935–54.
15. Schawe JEK. Investigations of the glass transitions of organic and inorganic substances: DSC and temperature-modulated DSC. *J Therm Anal.* 1996;47:475–84.
16. Hensel A, Schick C. Relation between freezing-in due to linear cooling and the dynamic glass transition temperature by temperature-modulated DSC. *J Non-Cryst Solids.* 1998;235:510–6.
17. Hutchinson JM, Montserrat S. The application of temperature-modulated DSC to the glass transition region II. Effect of a distribution of relaxation times. *Thermochim Acta.* 2001;377:63–84.
18. Donth E. The glass transition. Relaxation dynamics in liquids and disordered materials. Berlin: Springer; 2001.
19. Montserrat S, Calventus Y, Hutchinson JM. Effect of cooling rate and frequency on the calorimetric measurement of the glass transition. *Polymer.* 2005;46:12181–9.

20. Tool AQ. Relation between inelastic deformability and thermal expansion of glass in its annealing range. *J Am Ceram Soc.* 1946;29:240–53.
21. Richardson MJ, Savill NG. Derivation of accurate glass-transition temperatures by differential scanning calorimetry. *Polymer.* 1975;16:753–7.
22. Moynihan CT, Eastal AJ, DeBolt MA, Tucker J. Dependence of fictive temperature of glass on cooling rate. *J Am Ceram Soc.* 1976;59:12–6.
23. Hodge IM. Enthalpy relaxation and recovery in amorphous materials. *J Non-Cryst Solids.* 1994;169:211–66.
24. Narayanaswamy OS. Model of structural relaxation in glass. *J Am Ceram Soc.* 1971;54:491–8.
25. Vogel H. Das Temperaturabhängigkeitsgesetz der Viskosität von Flüssigkeiten. *Physik Z.* 1921;22:645–6.
26. Fulcher GS. Analysis of recent measurements of the viscosity of glasses. *J Am Ceram Soc.* 1925;8:339–55.
27. Tammann G, Hesse W. Die Abhängigkeit der Viskosität von der Temperatur bei unterkühlten Flüssigkeiten. *Z anorg Allgem Chem.* 1926;156:245–51.
28. Angell CA. Strong and fragile liquids. In: Ngai KL, Wright GB, editors. *Relaxations in complex systems.* Springfield, VA: US Department of Commerce; 1984. p. 3–11.
29. Chryssikos GD, Duffy JA, Hutchinson JM, Ingram MD, Kamitsos EI, Pappin AJ. Lithium borate glasses: a quantitative study of strength and fragility. *J Non-Cryst Solids.* 1994;172:378–83.
30. Sokolov AP, Novikov VN, Ding Y. Why many polymers are so fragile. *J Phys Condens Matter* 2007;19:Art. No. 205116 (8 pp).
31. Hutchinson JM. Interpretation of glass transition phenomena in the light of the strength-fragility concept. *Polym Int.* 1998;47:56–64.
32. Adam G, Gibbs JH. On the temperature dependence of cooperative relaxation properties in glass-forming liquids. *J Chem Phys.* 1965;43:139–46.
33. Hutchinson JM, Montserrat S, Calventus Y, Cortés P. Application of the Adam-Gibbs equation to the non-equilibrium glassy state. *Macromolecules.* 2000;33:5252–62.
34. Gibbs JH, DiMarzio EA. Nature of the glass transition and the glassy state. *J Chem Phys.* 1958;28:373–83.
35. Doolittle AK. Studies in Newtonian flow. 2. The dependence of the viscosity of liquids on free space. *J Appl Phys.* 1951;22:1471–5.
36. Kovacs AJ, Hutchinson JM, Aklonis JJ. Isobaric volume and enthalpy recovery of glasses. (I). A critical survey of recent phenomenological approaches. In: Gaskell PH, editor. *The structure of non-crystalline materials.* London: Taylor and Francis; 1977. p. 153–63.
37. Pappin AJ, Hutchinson JM, Ingram MD. Enthalpy relaxation in polymer glasses: evaluation and interpretation of the Tool-Narayanaswamy parameter  $x$  for poly(vinyl chloride). *Macromolecules.* 1992;25:1084.
38. Montserrat S, Cortés P, Pappin AJ, Quah KH, Hutchinson JM. Structural relaxation in fully cured epoxy resins. *J Non-Cryst Solids.* 1994;172:1017–22.
39. Hutchinson JM, Ruddy M, Wilson MR. Differential scanning calorimetry of polymer glasses: corrections for thermal lag. *Polymer.* 1988;29:152–9.
40. Kovacs AJ. La contraction isotherme du volume des polymères amorphes. *J Polym Sci.* 1958;30:131–47.
41. Slobodian P, Riha P, Rychwalski RW, Emri I, Saha P, Kubát J. The relation between relaxed enthalpy and volume during physical aging of amorphous polymers and selenium. *Eur Polym J.* 2006;42:2824–37.
42. Hadac J, Slobodian P, Riha P, Saha P, Rychwalski RW, Emri I, et al. Effect of cooling rate on enthalpy and volume relaxation of polystyrene. *J Non-Cryst Solids.* 2007;353:2681–91.
43. Malek J. Volume and enthalpy relaxation rate in glassy materials. *Macromolecules.* 1998;31:8312–22.
44. Malek J, Mitsuhashi T. Comparison between volume and enthalpy relaxations in non-crystalline solids based on the fictive relaxation rate. *J Therm Anal Calorim.* 1999;57:707–16.
45. Svoboda R, Pustkova P, Malek J. Volume relaxation of a-Se studied by mercury dilatometry. *J Non-Cryst Solids.* 2006;352:4793–9.
46. Svoboda R, Pustkova P, Malek J. Structural relaxation of polyvinyl acetate (PVAc). *Polymer.* 2008;49:3176–85.
47. Petrie SEB. Thermal behavior of annealed organic glasses. *J Polym Sci Pt A2.* 1972;10:1255–72.
48. Sasabe H, Moynihan CT. Structural relaxation in polyvinyl acetate. *J Polym Sci Polym Phys.* 1978;16:1447–57.
49. Perez J, Cavaille JY, Calleja RD, Ribelles JLG, Pradas MM, Greus AR. Physical aging of amorphous polymers: theoretical analysis and experiments on poly(methyl methacrylate). *Makromol Chem.* 1991;192:2141–61.
50. Adachi K, Kotaka T. Volume and enthalpy relaxation in polystyrene. *Polym J.* 1982;14:959–70.
51. Simon SL, Plazek DJ, Sobieski JW, McGregor ET. Physical aging of a polyetherimide: volume recovery and its comparison to creep and enthalpy measurements. *J Polym Sci Polym Phys.* 1997;35:929–36.
52. Simon SL, Sobieski JW, Plazek DJ. Volume and enthalpy recovery of polystyrene. *Polymer.* 2001;42:2555–67.
53. Számel G, Klebert S, Sajó I, Pukanszky B. Thermal analysis of cellulose acetate modified with caprolactone. *J Therm Anal Calorim.* 2008;91:715–22.
54. Cook WD, Scott TF, Quay-Thevenon S, Forsythe JS. Dynamic mechanical thermal analysis of thermally stable and thermally reactive network polymers. *J Appl Polym Sci.* 2004;93:1348–59.
55. Kelly A, Hine PJ, Landert M, Ward IM. The effect of the measurement frequency on the elastic anisotropy of fibre laminates. *J Mater Sci.* 2005;40:4461–7.
56. Cook WD, Chen F, Pattison DW, Hopson P, Beaujon M. Thermal polymerization of thiolene network-forming systems. *Polym Int.* 2007;56:1572–9.
57. Delin M, Rychwalski RW, Kubát J, Klason C, Hutchinson JM. Physical aging time scales and rates for poly(vinyl acetate) stimulated mechanically in the T<sub>g</sub> region. *Polym Eng Sci.* 1996;36:2955–67.
58. Lionetto F, Maffezzoli A. Relaxations during the post-cure of unsaturated polyester networks by ultrasonic wave propagation, dynamic mechanical analysis, and dielectric analysis. *J Polym Sci Polym Phys.* 2005;43:596–602.
59. Montserrat S. Vitrification and physical aging on isothermal curing of an epoxy resin. *J Therm Anal.* 1991;37:1751–8.
60. Cassettari M, Salvetti G, Tombari E, Veronesi S, Johari GP. Calorimetric determination of vitrification time and heat capacity of a thermosetting polymer. *J Polym Sci Polym Phys.* 1993;31:199–205.
61. Van Assche G, Van Hemelrijck A, Raier H, Van Mele B. Modulated differential scanning calorimetry: isothermal cure and vitrification of thermosetting systems. *Thermochim Acta.* 1995;268:121–42.
62. Van Hemelrijck A, Van Mele B. Modulated temperature differential scanning calorimetry: characterization of curing systems by TTT and CHT diagrams. *J Therm Anal.* 1997;49:437–42.
63. Montserrat S, Cima I. Isothermal curing of an epoxy resin by alternating differential scanning calorimetry. *Thermochim Acta.* 1999;330:189–200.
64. Montserrat S, Pla X. Use of temperature-modulated DSC in kinetic analysis of a catalysed epoxy-anhydride system. *Polym Int.* 2004;53:326–31.
65. Hutchinson JM. Characterising the glass transition and relaxation kinetics by conventional and temperature-modulated differential scanning calorimetry. *Thermochim Acta.* 1998;324:165–74.

66. Hutchinson JM. Studying the glass transition by DSC and TMDSC. *J Therm Anal Calorim.* 2003;72:619–29.
67. Fraga I, Montserrat S, Hutchinson JM. Vitrification during the isothermal cure of thermosets. Part I. An investigation using TOPEM, a new temperature modulated technique. *J Therm Anal Calorim.* 2008;91:687–95.
68. Fraga I, Montserrat S, Hutchinson JM. Vitrification during the isothermal cure of thermosets: comparison of theoretical simulations with temperature-modulated DSC and dielectric analysis. *Macromol Chem Phys.* 2008;209:2003–11.
69. Hutchinson JM, Montserrat S. The application of modulated differential scanning calorimetry to the glass transition: theoretical analysis using a single parameter model. *J Therm Anal.* 1996;47:103–15.
70. Hutchinson JM, Montserrat S. The application of modulated differential scanning calorimetry to the glass transition of polymers. I. A single-parameter theoretical model and its predictions. *Thermochim Acta.* 1996;286:263–96.
71. Hutchinson JM, Montserrat S. A theoretical model of temperature-modulated differential scanning calorimetry in the glass transition region. *Thermochim Acta.* 1997;304:257–65.
72. Montserrat S, Hutchinson JM. On the measurement of the width of the distribution of relaxation times in polymer glasses. *Polymer.* 2002;43:351–5.
73. Jiang Z, Hutchinson JM, Imrie CT. Temperature-modulated differential scanning calorimetry. Part II. Determination of activation energies. *Polym Int.* 1998;47:72–5.
74. Schawe JEK, Hütter T, Heitz C, Alig I, Lelliger D. Stochastic temperature modulation: a new technique in temperature-modulated DSC. *Thermochim Acta.* 2006;446:147–55.
75. Donth E, Korus J, Hempel E, Beiner M. Comparison of DSC heating rate and HCS frequency at the glass transition. *Thermochim Acta.* 1997;304:239–49.
76. Weyer S, Hensel A, Korus J, Donth E, Schick C. Broad band heat capacity spectroscopy in the glass-transition region of polystyrene. *Thermochim Acta.* 1997;304:251–5.
77. Weyer S, Merzlyakov M, Schick C. Application of an extended Tool–Narayanaswamy–Moynihan model. Part 1. Description of vitrification and complex heat capacity measured by temperature-modulated DSC. *Thermochim Acta.* 2001;377:85–96.
78. Weyer S, Huth H, Schick C. Application of an extended Tool–Narayanaswamy–Moynihan model. Part 2. Frequency and cooling rate dependence of glass transition from temperature modulated DSC. *Polymer.* 2005;46:12240–6.
79. Donth E. The size of the cooperatively rearranging regions at the glass transition. *J Non-Cryst Solids.* 1982;53:325–30.
80. Kovacs AJ, Aklonis JJ, Ramos AR, Hutchinson JM. Isobaric volume and enthalpy recovery of glasses. II. A transparent multiparameter theory. *J Polym Sci Polym Phys.* 1979;17:1097–162.
81. Ngai KL. Universality of low-frequency fluctuation, dissipation and relaxation properties of condensed matter. I. Comments on *Solid State Phys.* 1979;9:127–40.
82. Ngai KL. Universality of low-frequency fluctuation, dissipation and relaxation properties of condensed matter. II. Comments on *Solid State Phys.* 1980;9:141–55.
83. Ngai KL, Rendell RW, Rajagopal AK, Teitler S. Three coupled relations for relaxations in complex systems. *Ann N Y Acad Sci.* 1986;484:150–84.
84. Danch A. Some comments on nature of the structural relaxation and glass transition. *J Therm Anal Calorim.* 2008;91:733–6.
85. Tracht U, Wilhelm M, Heuer A, Feng H, Schmidt-Rohr K, Spiess HW. Length scale of dynamic heterogeneities at the glass transition determined by multidimensional nuclear magnetic resonance. *Phys Rev Lett.* 1998;81:2727–30.
86. Russell EV, Israeloff NE. Direct observation of molecular cooperativity near the glass transition. *Nature.* 2000;408:695–8.
87. Tyagi M, Alegria A, Colmenero J. Heterogeneous dynamics of poly(vinyl acetate) far above T<sub>g</sub>: a combined study by dielectric spectroscopy and quasi-elastic neutron scattering. *J Chem Phys.* 2005;122:244909. (13 pp).
88. Huth H, Beiner M, Weyer S, Merzlyakov M, Schick C, Donth E. Glass transition cooperativity from heat capacity spectroscopy: temperature dependence and experimental uncertainties. *Thermochim Acta.* 2001;377:113–24.
89. Donth E. Characteristic length of the glass transition. *J Polym Sci Polym Phys.* 1996;34:2881–92.
90. Schröter K. Characteristic length of glass transition heterogeneity from calorimetry. *J Non-Cryst Solids.* 2006;352:3249–54.